Composites: Part B 43 (2012) 2646–2654

Contents lists available at SciVerse ScienceDirect

Composites: Part B

journal homepage: www.elsevier.com/locate/compositesb

Influence of pattern gradation on the design of piezocomposite energy harvesting devices using topology optimization

S.L. Vatanabe [a], G.H. Paulino [b], E.C.N. Silva [a,*]

[a] Department of Mechatronics and Mechanical Systems Engineering, Polytechnic School of University of São Paulo, SP, Brazil
[b] Newmark Laboratory, Department of Civil and Environmental Engineering, University of Illinois at Urbana-Champaign, IL, USA

ARTICLE INFO

Article history:
Received 12 December 2011
Received in revised form 24 March 2012
Accepted 29 March 2012
Available online 13 April 2012

Keywords:
A. Ceramic–matrix composites (CMCs)
A. Polymer–matrix composites (PMCs)
C. Finite element analysis (FEA)
B. Electrical properties
Topology optimization

ABSTRACT

Piezoelectric materials can be used to convert oscillatory mechanical energy into electrical energy. Energy harvesting devices are designed to capture the ambient energy surrounding the electronics and convert it into usable electrical energy. The design of energy harvesting devices is not obvious, requiring optimization procedures. This paper investigates the influence of pattern gradation using topology optimization on the design of piezocomposite energy harvesting devices based on bending behavior. The objective function consists of maximizing the electric power generated in a load resistor. A projection scheme is employed to compute the element densities from design variables and control the length scale of the material density. Examples of two-dimensional piezocomposite energy harvesting devices are presented and discussed using the proposed method. The numerical results illustrate that pattern gradation constraints help to increase the electric power generated in a load resistor and guides the problem toward a more stable solution.

© 2012 Elsevier Ltd. All rights reserved.

1. Introduction

The direct and converse piezoelectric effects of certain active materials have been employed in numerous applications of energy harvesting devices, with the goal of reducing or eliminating the need for external power sources or batteries in electronic devices in general. The interest in vibrational energy harvesting has been motivated by advances in low-power electronic components such as wireless sensors for structural health monitoring and tire pressure sensors, actuators that can be powered remotely, and by the need for supplemental energy sources for unmanned aerial vehicles [1]. Additional motivation is provided by the desire to develop such devices with simultaneous structural and power generation functionality, which can reduce weight, material usage, and costs. The interest in piezoelectric energy harvesting is reflected in a number of authoritative reviews that have been written in recent years [2–4].

Piezoelectric material can be combined with other non-piezoelectric materials, generating new types of materials, called piezocomposites. These materials usually offer substantial advantages over conventional piezoelectric materials, such as high electromechanical coupling and better energy conversion [5]. Piezocomposite energy harvesting devices can be designed for quasi-static applications, where the excitation frequency is much lower than the resonance frequency, or for dynamic applications, where the goal is to operate the device in a frequency range as close as possible to a determined resonance frequency. In quasi-static applications, usually the goal is to maximize the conversion of mechanical energy into electricity, which can be measured by various criteria, however, the electromechanical coupling coefficient k is most commonly used. In the case of dynamic applications, the goal is to directly maximize the electrical power generated in a given load [6]. Zhu et al. [7] used a cantilever with a sandwich structure and a seismic mass attached to the tip to analyze the power output of a vibration-based piezoelectric energy-harvesting device when it is connected to a load resistor. They found that the series or parallel configurations of the piezoelectric layers can change the distribution of the electric current and voltage at the output terminals. However, it cannot change significantly the power output and vibrational amplitude when the structure is subjected to the same excitations.

Topology optimization is a computational technique used for determining the layout, or topology, of a structure or material such that a prescribed objective is maximized or minimized, subjected to design constraints. It has been successfully applied to design piezoelectric devices in recent years. Silva et al. [5,8,9] used topology optimization and homogenization for designing piezoelectric microstructures with high performance characteristics, such as hydrostatic coupling coefficient, figure of merit, and electromechanical coupling factor. Sigmund et al. [10] employed topology optimization to design 1–3 piezocomposites with

* Corresponding author.
E-mail address: ecnsilva@usp.br (E.C.N. Silva).

1359-8368/$ - see front matter © 2012 Elsevier Ltd. All rights reserved.
http://dx.doi.org/10.1016/j.compositesb.2012.03.023

optimal performance characteristics for hydrophone applications. Buehler et al. [11] applied homogenization to calculate the effective properties of an unit cell incorporating piezoelectric and conventional materials. They maximize the displacement of an arbitrary point due to an applied electric field, while specifying the structure strength. Jayachandran et al. [12–14] used stochastic global optimization combined with homogenization to obtain the optimal granular configuration of ferroelectric ceramic microstructure for application in piezoelectric actuators.

Topology optimization has also been applied to design piezoelectric energy harvesting devices, by distributing piezoelectric material and others in a given design domain, in order to maximize the output electric power. Zheng et al. [15] applied the topology optimization method to design piezoelectric energy harvesting devices, by maximizing the converted electric energy, considering static applications. Rupp et al. [6] developed a computational approach to design dynamic piezoelectric energy harvesting systems composed of layered plates and shells connected to an electrical circuit. They found that a design methodology solely based on finding regions of positive and negative strain is inadequate for design purposes when the piezoelectric layers significantly change the structural response. Chen et al. [16] proposed a level set-based topology optimization approach to synthesize mechanical energy harvesting devices for self-powered micro systems by reformulating the energy harvester design problem as a PDE-constrained topology optimization problem. Nakasone and Silva [17] presented a formulation for dynamic design of piezoelectric laminated plates aiming at piezoelectric sensors, actuators and energy-harvesting applications. Through this formulation, a design with enhanced energy conversion in the low-frequency spectrum is obtained, by minimizing a set of first eigenvalues, enhancing their corresponding eigenshapes while maximizing their electromechanical coupling coefficients. Lee and Youn [18] explored the segmentation of a piezoelectric material layer, guided by inflection lines from multiple vibration modes of interest to minimize voltage cancellation. El-Sabbagh and Baz [19] investigated the use of multiple pairs of electrodes to overcome the problem of charge cancellation in piezoelectric bimorphs applied to energy harvesting applications.

The method presented in this work addresses the design of piezoelectric energy harvesters by tailoring the layout of piezocomposite structures. In this work, the influence of pattern gradation [20] is investigated in the design of dynamic piezocomposite energy harvesting devices by means of the topology optimization method. New parameters are included in the investigation, such as the number of patterns in the design domain and the variation of dimensions of the pattern along the structure. This approach has the potential to improve the design of dynamic piezoelectric energy harvesters by tailoring the layout of piezocomposite structures, aiming at maximization of electric power generated in the load resistor and at guiding the problem toward to a more stable result.

In order to ensure convergence upon mesh refinement, the application of filtering techniques have been popular. Filtering techniques originally comprised sensitivity filtering [21] and density filtering [22], and these two approaches have produced globally convergent mesh designs that, in many cases, are satisfactory for practical purposes. Recently, a number of projection schemes that alleviate the gray transition problem have been proposed by Guest et al. [23], Sigmund [24], Xu et al. [25], Kawamoto et al. [26], among others [27,28]. In the present work, a projection technique is implemented to avoid mesh dependency and checkerboard patterns, and a random initial material distribution is considered in order to avoid local minima, a common problem in the design of optimized dynamic structures.

This paper is organized as follows: in Section 2, the mechanical, piezoelectric, circuit modelling, and corresponding formulation using the finite element method are described. In Section 3, the topology optimization formulation is provided. In Section 4, the numerical implementation of the pattern gradation concept is explained, in conjunction with the different design domains adopted in this work. In Section 5, numerical examples demonstrating the influence of the pattern gradation concept in the design of dynamic piezocomposite energy harvesting devices are shown. Finally, in Section 6, some conclusions are inferred.

2. Piezoelectric finite element method for dynamic applications

The analysis tool adopted in this paper is the Finite Element Method (FEM), mainly because each individual element can be manipulated as a single entity within the complex system. This is an important issue in the topology optimization method, once each finite element depends on a local group of design variables.

The displacement and electric potentials are assumed to have harmonic behavior, i.e.

$$\mathbf{U} = \mathbf{U}_e e^{i\omega t}, \quad \mathbf{\Phi} = \mathbf{\Phi}_e e^{i\omega t} \tag{1}$$

respectively. The piezoelectric dynamic system with structural damping and load resistor can be written in the finite element form as follows

$$-\omega^2 \begin{bmatrix} \mathbf{M} & \mathbf{0} \\ \mathbf{0} & \mathbf{0} \end{bmatrix} \begin{Bmatrix} \mathbf{U} \\ \mathbf{\Phi} \end{Bmatrix} + i\omega \left(\begin{bmatrix} \mathbf{C} & \mathbf{0} \\ \mathbf{0} & \mathbf{0} \end{bmatrix} + \begin{bmatrix} \mathbf{0} & \mathbf{0} \\ \mathbf{0} & \mathbf{K}_R \end{bmatrix} \right) \begin{Bmatrix} \mathbf{U} \\ \mathbf{\Phi} \end{Bmatrix} + \begin{bmatrix} \mathbf{K_{uu}} & \mathbf{K_{u\phi}} \\ \mathbf{K}_{\mathbf{u}\phi}^t & \mathbf{K}_{\phi\phi} \end{bmatrix} \begin{Bmatrix} \mathbf{U} \\ \mathbf{\Phi} \end{Bmatrix} = \begin{Bmatrix} \mathbf{F} \\ \mathbf{Q} \end{Bmatrix} \tag{2}$$

where $\mathbf{M}$, $\mathbf{C}$, $\mathbf{K}_R$, $\mathbf{K_{uu}}$, $\mathbf{K_{u\,\phi}}$ and $\mathbf{K}_{\phi\phi}$ are the mass, damping, load resistor, stiffness, piezoelectric, and dielectric matrices, respectively, and $\mathbf{U}$, $\mathbf{\Phi}$, $\mathbf{F}$ and $\mathbf{Q}$ are the displacement, electric potential, force, and electric charge vectors, respectively. Notice that $\mathbf{U}$ and Φ are complex vectors.

The structural damping matrix adopted here is defined by

$$\mathbf{C} = \beta \mathbf{K_{uu}} \tag{3}$$

where β is the damping factor. It is possible to add a proportional mass matrix $\mathbf{M}$ to compute $\mathbf{C}$. However, usually, energy harvesting devices operate in the first or second resonance frequency, and thus, the influence of $\mathbf{M}$ in damping model is negligible when the model is excited at low frequencies. Therefore, in this work, $\mathbf{C}$ is considered proportional to $\mathbf{K_{uu}}$ only. The load resistor matrix, in harmonic analysis, is obtained by

$$\mathbf{K}_R = \left(-\frac{1}{\omega^2 R} \right) \begin{bmatrix} 1 & -1 \\ -1 & 1 \end{bmatrix} \begin{Bmatrix} \phi_1 \\ \phi_2 \end{Bmatrix} \tag{4}$$

where ϕ_1 and ϕ_2 are the degrees of freedom of electric potential where the resistor is coupled.

The electric power P generated in the resistor R is obtained by

$$P = \frac{V_{rms}^2}{R} = \frac{(\Delta\phi_{peak})^2}{2R} \tag{5}$$

where V_{rms} is the RMS voltage calculated between the electrodes. The electromechanical coupling coefficient (k) measures the conversion of mechanical energy into electricity and it is calculated by [5]:

$$k^2 = \frac{(\text{Electromechanical Energy})^2}{(\text{Mechanical Energy})(\text{Electrical Energy})} = \frac{(\mathbf{U}^t \mathbf{K}_{\mathbf{u}\phi} \mathbf{\Phi})^2}{(\mathbf{U}^t \mathbf{K_{uu}} \mathbf{U})(\mathbf{\Phi}^t \mathbf{K}_{\phi\phi} \mathbf{\Phi})} \tag{6}$$

3. Topology optimization formulation

The optimization consists in distributing the material within a design domain to maximize (or minimize) a desired objective

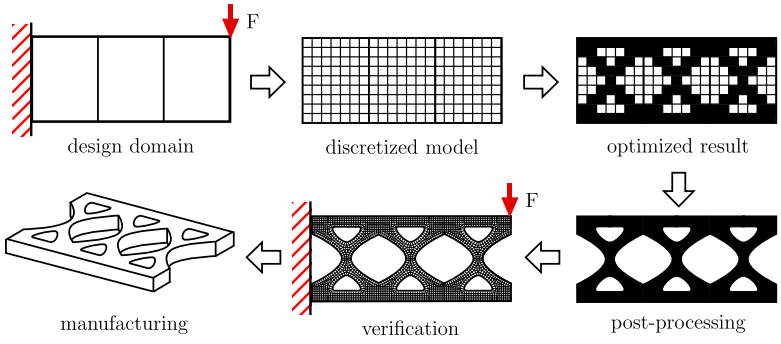

Fig. 1. Steps of piezoelectric devices design using topology optimization.

function. The steps of the design of piezoelectric devices using the topology optimization method are shown in Fig. 1. Loads, boundary conditions and constraints are applied to the design domain, which is discretized into finite elements. The optimization iterative process is carried out until it has obtained an optimized material distribution. Then, it is performed the post-processing step, where the optimized result is interpreted, verified and sent to manufacturing.

3.1. Material model

The discrete problem, where the amount of material at each element can assume only values equal to either one or zero is an ill-posed problem. A typical way to seek a solution for topology optimization problems is to relax the problem by allowing the material to assume intermediate property values during the optimization procedure, which can be achieved by defining a special material model [29,30]. Thus, in this work, the topology optimization formulation employs a material model based on the SIMP (Solid Isotropic Material With Penalization) [31]. The traditional SIMP model states that at each point of the domain, the local effective property Ψ_H of the mixture is

$$\Psi_H = \rho^p \Psi_B + (1-\rho^p)\Psi_A \tag{7}$$

where Ψ_A and Ψ_B are the constituent material properties and p is the penalization coefficient. Ψ_A and Ψ_B correspond to the elastic ($\mathbf{c}^E$), piezoelectric ($\mathbf{e}$) and dielectric ($\boldsymbol{\varepsilon}^S$) properties. The variable ρ is a pseudo-density describing the amount of material at each point of the domain, which can assume values between 0 and 1.

Essentially, this material model approximates the material distribution by defining a function of a continuous parameter (design variable) that determines the mixture of basic materials throughout the domain. In this sense, the relaxation yields a continuous material design problem that no longer involves a discernible connectivity. A topology solution can be obtained by applying penalization coefficients p to the material model to recover the $0-1$ design. In this work, $p = 3$ is adopted.

4. Numerical implementation

The discrete formulation problem is defined by:

$$\begin{aligned} &\underset{\mathbf{d}}{Maximize}: && P \\ &subjected\ to: && \text{equilibrium equation} \\ & && 0 \leqslant \mathbf{d} \leqslant 1 \\ & && V(\mathbf{d}) = \sum_{i=1}^{N} \mathbf{d}\, d\Omega \leqslant V_s \end{aligned}$$

where $\mathbf{d}$ are the design variables of each element. To avoid numerical problems that arise in the implementation of the topology optimization method, such as mesh dependency and checkerboard instability, a projection technique, based on the work of Stromberg et al. [20], is implemented. The optimization problem is solved using the MMA solver (*Method of Moving Asymptotes*) [32].

4.1. Pattern gradation in one direction

The pattern repetition is defined as the number of times a particular pre-defined region, called pattern, is repeated along the domain, in one or more directions. The gradation consists of geometrically modifying (stretching or shrinking) one or more dimensions of each repetition along the domain [20].

In this work, the implementation of the pattern gradation constraint is based on MTOP ("Multiresolution Topology Optimization"), as presented by Nguyen et al. [33]. The MTOP concept considers the design variable mesh separated from the finite element mesh (see Fig. 2). Thus, a layer of pseudo-densities are added to the model, which are function of the design variables according to a projection method.

Once the pattern gradation parameters are defined, such as the number of patterns in the domain and the adopted gradation, design variables are distributed in the largest pattern, which are considered primary design variables, as shown in gray in Fig. 3. These variables are mapped in the repeated regions, originating the mapped design variables, shown in black in Fig. 3. This figure also shows the pattern being shrunk along the domain by the background gradient color.[1]

For a pattern gradation in one direction, the pattern is defined by the region enclosed by two coordinates, denoted by x_{n-1} and x_n, for the n-th pattern. In Fig. 3, for example, the pattern gradation is performed in the x-direction. Thus, pattern 1 is specified by selecting the coordinates x_0 and x_1 as bounds. This concept is carried over for each of the n patterns and the mapped variables at each repetition are correlated to the primary design variables. The mapped design variables are defined as follows [20]:

$$x^* = \sum_{i=0}^{n-1}(x_{i+1} - x_i) + \alpha_n(x - x_n) \tag{8}$$

where α is a scaling parameter of the n-th pattern with respect to the biggest pattern (which are the primary design variables). This scaling parameter is defined by:

$$\alpha_n = \frac{x_{n+1} - x_n}{x_1 - x_0} \tag{9}$$

The mapped design variables have the same values of the respective primary design variables values, so the solver adopted in topology optimization only modifies the values of the primary design variables.

[1] For interpretation of color in Figs. 1–4 and 6–13, the reader is referred to the web version of this article.

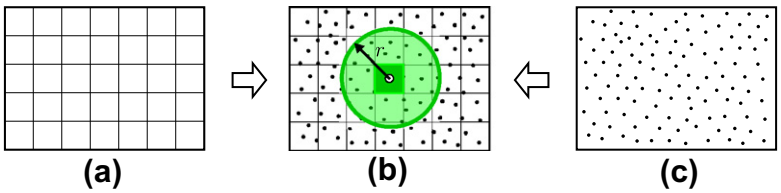

Fig. 2. Illustration of MTOP concept: (a) finite element mesh; (b) pseudo-density mesh and (c) design variable mesh [20].

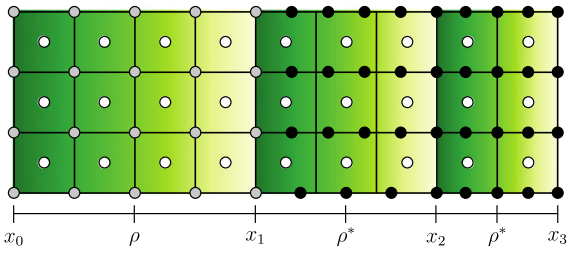

Fig. 3. Example of pattern gradation in one direction; primary design variables are indicated in gray, mapped design variables in black, and the gradation is indicated by the background gradient color [20].

The weighting factors of the projection function must be reformulated for the pattern gradation. Thus, the projection area is no longer circular and it can assume an elliptical shape, depending on the position of each element. The larger dimension of the ellipse can measure $2r_{min}$ and the distances between nodes are multiplied by the scaling parameter α (see Fig. 4c). In regions near of the boundaries of the domain, the projection area assumes a hybrid form of circle and ellipse (see Fig. 4b). The weighting factors are calculated as follows [20]:

$$w_j^e = \begin{cases} \frac{r_{\min} - r_j^e}{r_{\min}} & \text{if } r \leqslant r_{\min} \\ 0 & \text{if } r > r_{\min} \end{cases} \tag{10}$$

where w_j^e is the node weight j of element e, r_j^e defines the distance between the centroid of element e and the node j in the projection area Ω_e. The calculus of r_j^e is defined by

$$r_j^e = \begin{cases} x_j - x_e & x_j \in \Omega_e, x_0 \leqslant x_j \leqslant x_1, x_0 \leqslant x_e \leqslant x_1 \\ \frac{(x_j - x_1)}{\alpha_n} + (x_1 - x_e) & x_j \in \Omega_e, x_1 < x_j, x_0 \leqslant x_e \leqslant x_1 \\ \frac{(x_e - x_1)}{\alpha_n} + (x_1 - x_j) & x_j \in \Omega_e, x_1 < x_e, x_0 \leqslant x_j \leqslant x_1 \\ \frac{(x_j - x_e)}{\alpha_n} & x_j \in \Omega_e, x_1 < x_j, x_1 < x_e \\ 0 & \text{otherwise} \end{cases} \tag{11}$$

Each pseudo-density is calculated by

$$\rho_e = \frac{\sum_{j \in \Omega_e} w_j^e \rho_j^e}{\sum_{j \in \Omega_e} w_j^e} \tag{12}$$

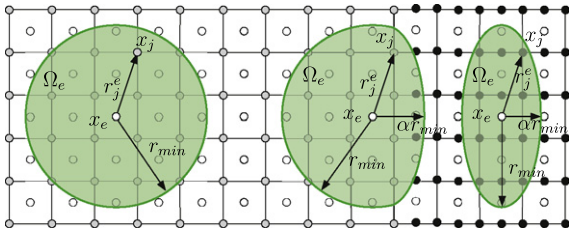

Fig. 4. Example of different projection areas along the domain.

4.2. Sensitivities

By using the MMA algorithm as the optimization solver, it is necessary to evaluate the sensitivities of the objective functions with respect to the design variables. In this section, the expressions for the sensitivities with respect to a general design variable ρ (which can be substituted by the design variables d) are presented. The electric power presented in Eq. (5) can be written by the following form:

$$P = \frac{\left(\mathbf{L}_{dummy}^T \mathbf{\Phi}\right)^2}{2R} \tag{13}$$

where $\mathbf{L}_{dummy}$ is a dummy global vector with a positive unitary value at one electrode and a negative unitary value at the other electrode. The negative value is due to the voltage difference of the formula. Considering that $\frac{\partial \mathbf{F}}{\partial \rho_i} = \mathbf{0}$ and $\mathbf{Q} = \mathbf{0}$, the sensitivity of the objective function (Eq. (5)) yields to [6]:

$$\begin{aligned} \frac{\partial P}{\partial \rho_i} &= \left(\frac{\mathbf{L}_{dummy}^T \mathbf{\Phi}}{R}\right) \left\{ \mathbf{0} \quad \mathbf{L}_{dummy}^T \right\} \begin{Bmatrix} \frac{\partial \mathbf{U}}{\partial \rho_i} \\ \frac{\partial \mathbf{\Phi}}{\partial \rho_i} \end{Bmatrix} \\ &= -\left(\frac{\mathbf{L}_{dummy}^T \mathbf{\Phi}}{R}\right) \left\{ \mathbf{0} \quad \mathbf{L}_{dummy}^T \right\} \mathbf{K}^{-1} \frac{\partial \mathbf{K}}{\partial \rho_i} \begin{Bmatrix} \mathbf{U} \\ \mathbf{\Phi} \end{Bmatrix} \\ &= -\left(\frac{\mathbf{L}_{dummy}^T \mathbf{\Phi}}{R}\right) \mathbf{L}_{adj}^T \frac{\partial \mathbf{K}}{\partial \rho_i} \begin{Bmatrix} \mathbf{U} \\ \mathbf{\Phi} \end{Bmatrix} \end{aligned} \tag{14}$$

where

$$\mathbf{K} = -\omega^2 \begin{bmatrix} \mathbf{M} & \mathbf{0} \\ \mathbf{0} & \mathbf{0} \end{bmatrix} + i\omega \left(\begin{bmatrix} \mathbf{C} & \mathbf{0} \\ \mathbf{0} & \mathbf{0} \end{bmatrix} + \begin{bmatrix} \mathbf{0} & \mathbf{0} \\ \mathbf{0} & \mathbf{K}_R \end{bmatrix} \right) + \begin{bmatrix} \mathbf{K}_{\mathbf{uu}} & \mathbf{K}_{\mathbf{u}\phi} \\ \mathbf{K}_{\mathbf{u}\phi} & \mathbf{K}_{\phi\phi} \end{bmatrix} \tag{15}$$

and

$$\frac{\partial \mathbf{K}}{\partial \rho_i} = \sum_N \left(-\omega^2 \frac{\partial}{\partial \rho_i} \begin{bmatrix} \mathbf{M}^e & \mathbf{0} \\ \mathbf{0} & \mathbf{0} \end{bmatrix} + i\omega \frac{\partial}{\partial \rho_i} \begin{bmatrix} \mathbf{C}^e & \mathbf{0} \\ \mathbf{0} & \mathbf{0} \end{bmatrix} + \frac{\partial}{\partial \rho_i} \begin{bmatrix} \mathbf{K}_{\mathbf{uu}}^e & \mathbf{K}_{\mathbf{u}\phi}^e \\ \mathbf{K}_{\mathbf{u}\phi}^e & \mathbf{K}_{\phi\phi}^e \end{bmatrix} \right) \tag{16}$$

The parameter N is the number of finite elements. The adjoint vector $\mathbf{L}_{adj}$ is used in order to avoid the inverse calculation of the matrix $\mathbf{K}$, which is obtained by solving the following linear system:

$$\mathbf{K}\mathbf{L}_{adj} = \begin{Bmatrix} \mathbf{0} \\ \mathbf{L}_{dummy} \end{Bmatrix} \tag{17}$$

This adjoint vector is calculated only one time per iteration, reducing the computational cost.

Once the pseudo-densities of each element are calculated based on the design variables, the calculation of sensitivity should be modified as follows:

$$\frac{\partial c}{\partial \rho_j^e} = \frac{\partial c}{\partial \rho_e} \frac{\partial \rho_e}{\partial \rho_j} = \frac{\partial c}{\partial \rho_e} \left(\frac{w_j^e}{\sum_{j \in \Omega_e} w_j^e} \right) \tag{18}$$

A flowchart of the optimization algorithm describing the steps involved is shown in Fig. 5. The software is implemented in MATLAB.

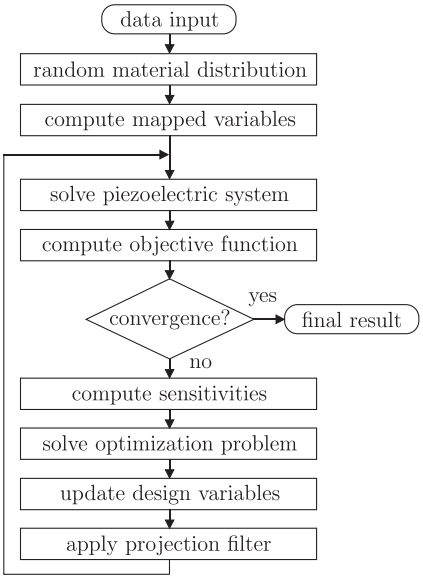

Fig. 5. Flowchart of the optimization procedure.

5. Numerical examples

The design domain adopted is shown in Fig. 6, whose dimensions are 100×20 mm. The piezoelectric layers are connected in parallel configuration. There is a resistor of 1 kΩ coupled to the electrodes and a harmonic unit force is applied to the free end of the design domain, with an excitation frequency of 1 kHz. The model assumes a plane strain state and it is symmetric about the x axis. The adopted materials are PZT-5A piezoceramic and epoxy polymer, whose properties are listed in Table 1. The structural damping parameter α has a value equal to 10^{-8}. The finite element mesh is discretized in 150×30 Q4 elements. Sensitivities are calculated using the adjoint method.

The design of dynamic structures may present many local minima, making difficult the design process of such devices. Thus, the main idea of this work is to evaluate the influence of pattern gradation in energy harvesting design. The adopted procedure consists of three different design domains, which are described below.

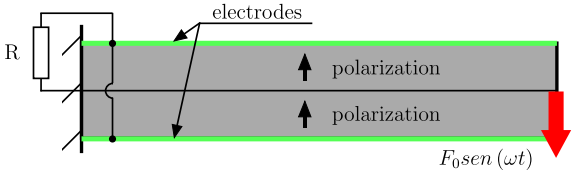

Fig. 6. Design domain adopted.

Table 1
Material properties.

Property	PZT-5A	Epoxy
c^E_{11} (10^{10}N/m^2)	12.1	0.53
c^E_{13} (10^{10}N/m^2)	7.52	0.31
c^E_{33} (10^{10}N/m^2)	11.1	0.53
c^E_{44} (10^{10}N/m^2)	2.10	0.11
e_{13} (C/m^2)	−5.4	0
e_{33} (C/m^2)	15.8	0
e_{15} (C/m^2)	12.3	0
$\varepsilon^S_{11}/\varepsilon_0$	1650	4
$\varepsilon^S_{33}/\varepsilon_0$	1700	4
Specific weight (kg/m^3)	7500	1384

5.1. Case 1: no pattern repetition

Fig. 7 illustrates the first case, where there is no pattern repetition. This case is used as a reference for the other two cases. This case has the largest solution space, once the solution spaces of the other two cases are contained in this solution space.

5.2. Case 2: with pattern repetition

Fig. 8 illustrates the second case, where it is imposed a pattern repetition, with no gradation between the patterns, i.e., all patterns have the same size (indicated in the dimension lines). This case has a smaller solution space than the case 1, because the available solutions are limited to those that have a topology with repeated patterns. In this case, the design variables are concentrated in the design domain indicated in Fig. 8 and the pseudo-density values under the design domain are symmetric with respect to the x axis. The pseudo-densities in the other patterns are mapped with respect to the first pattern.

5.3. Case 3: with pattern gradation

Fig. 9 illustrates the third case adopted, where it is imposed a pattern gradation in the domain. The adopted gradation ratio is given by 5, 4, 3, 2, and 1. These values mean that the first pattern is 5 times bigger than the last one, the second pattern is 4 times bigger than the last one, and so on.

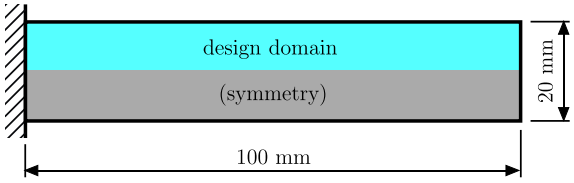

Fig. 7. Case 1: no pattern repetition.

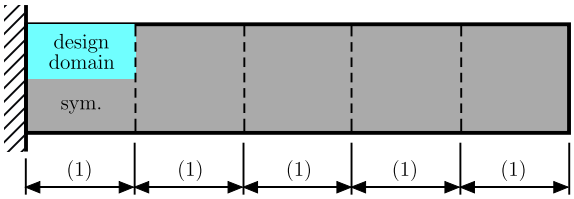

Fig. 8. Case 2: with pattern repetition.

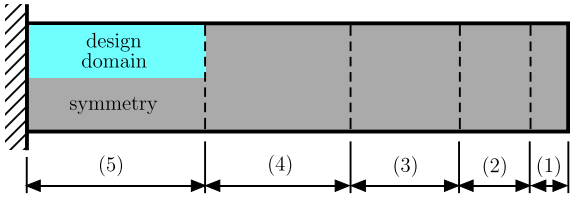

Fig. 9. Case 3: with pattern gradation.

5.4. Results and discussions

It is known that piezocomposite materials provides a better performance than pure piezoelectric materials. However, firstly a design domain of pure PZT-5A is simulated, shown in Fig. 13a, in order to serve as a reference for the other three cases. The first resonance frequency and the electric power generated in the load resistor are listed in the right side of the figure, which are 1020 Hz and 100 μW, when the structure is excited at an excitation frequency of 1000 Hz.

Regarding the choice of the initial material distributions, different initial guesses are tested (uniform distribution of materials, linear or circumferential gradation distribution along the design domain, among others). The procedure adopted in this work consists of using a set of 20 random initial material distributions. Approximately half of the simulations converge to the same result, which generates the highest electric power for this design domain (with no pattern repetition or gradation constraint). The other half (random initial material distributions) results in different topologies, which means that these topologies correspond to different local minima.

To clarify these issues, Fig. 10 shows the response of the electric power generated as a function of the excitation frequency for design domain with no pattern repetition. This figure shows three examples obtained from different random initial material distributions without using pattern repetition constraint, whose topologies differ dramatically. These three examples illustrate that the problem has many local minima.

In this chart it is also possible to notice the best solution obtained without pattern repetition (which generates 163 μW and it has the first resonance frequency at 1001 Hz) and the solution obtained by considering a slight variation of the design variable values. This slight variation is obtained in a subsequent iteration step from the best topology. This example shows that the dynamic optimization of the design domain with no pattern repetition is very sensitive to the design variables, having a negative impact in the convergence of the solution and leading to local minima. In fact, small variations in design variables may drastically change the behavior of the objective function. This problem is common when using gradient based optimization methods. In the example shown in the figure, a small variation of the optimized topology causes the electric power of 163 μW to decrease to less than 10 μW when the model is excited at 1000 Hz.

The same procedure is applied to the other two design domains with pattern repetition and pattern gradation – see Figs. 11 and 12, respectively. The proportion of topologies converging to the same result remains the same as before, i.e., about half of the simulations. These converged results are also those that generated the highest electric power for each case, as illustrated in Fig. 13.

Thus, considering pattern repetition or pattern gradation constraints, the problem becomes more stable, as seen in Figs. 11 and 12. Fig. 11 shows the response of the electric power as a function of the excitation frequency for the best topology obtained with pattern repetition constraint and for a topology considering a small variation of design variable values in relation to this topology. In this chart, it is easy to notice that both topologies present similar behavior, thus, facilitating the convergence of the problem. This same effect occurs in the case of the pattern gradation constraint, illustrated in Fig. 12. This means that the pattern repetition constraint can generate more stable solutions and helps to achieve better local minima.

The difference between the performance obtained with pattern repetition and pattern gradation constraint can be illustrated by the electromechanical coupling coefficient k (see Eq. (6)). Although more piezoelectric material is needed to convert the energy, its stiffness is too high, causing less deformation of the structure and, consequently, less energy is converted. On the contrary, flexible structures have less piezoelectric material, converting less energy. The best topology obtained using pattern repetition has a k equal to 0.098, whereas the best topology obtained using pattern gradation has a k equal to 0.139. These values show that more efficient energy conversion is obtained with the pattern gradation constraint.

All the obtained results are shown in Fig. 13b–d. The first resonance frequency and the electric power generated in the load resistor are listed by the side of each material distribution. For the first case, where no pattern repetition is considered, the first resonance frequency is 1001 Hz, which is very close to the excitation frequency, and the electric power generated is 163 μW, i.e., it is achieved a gain of 63% with respect to the pure PZT-5A. The second case analyzes the influence of patterns along the domain. The first resonance frequency is 999 Hz, which is also close to the excitation frequency, and the electric power is 152 μW, achieving a gain of 52% with respect to the pure PZT-5A. In the third case, where it is applied the pattern gradation constraint, the first

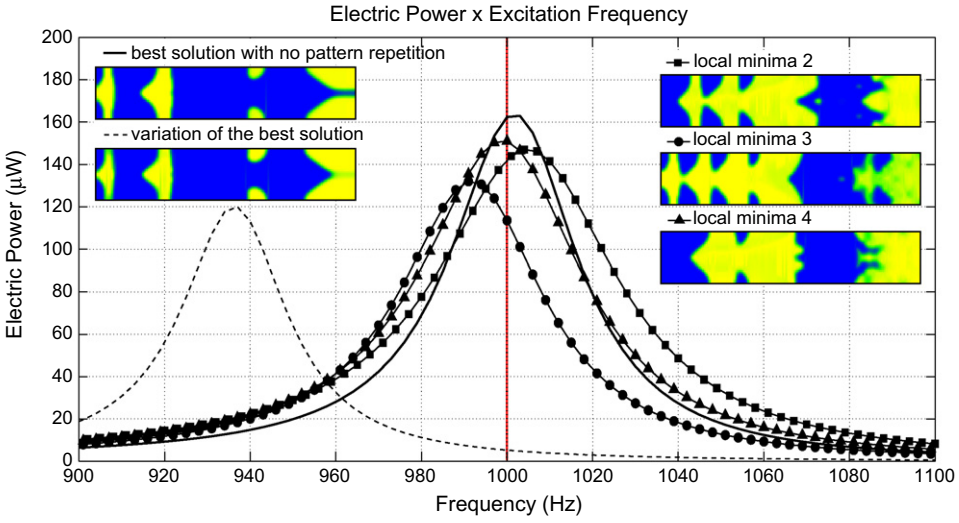

Fig. 10. Electric power as a function of the excitation frequency, for different local minima.

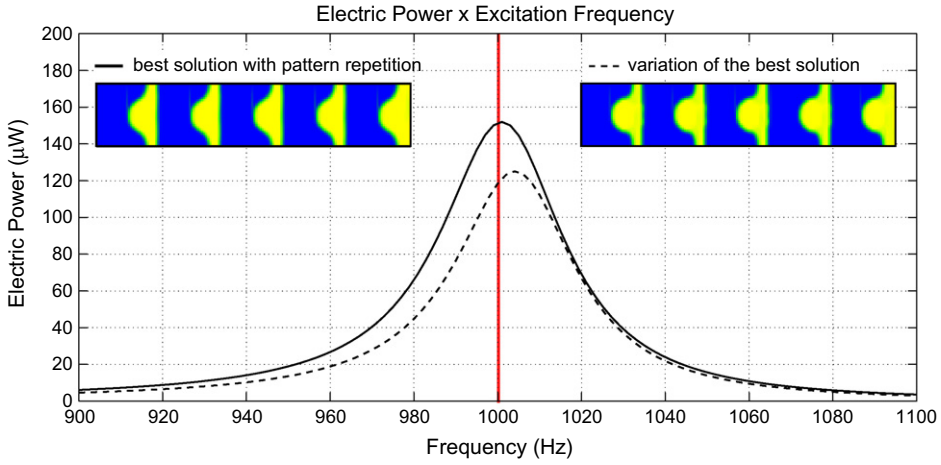

Fig. 11. Electric power as a function of the excitation frequency, for different local minima.

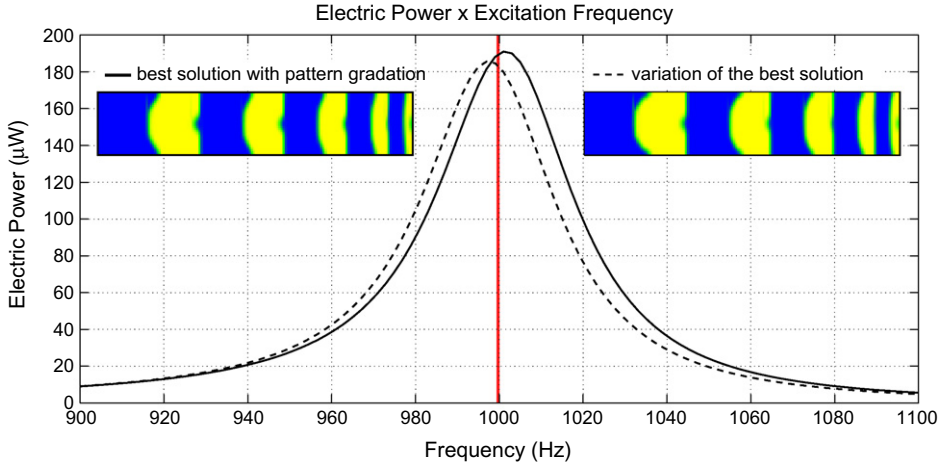

Fig. 12. Electric power as a function of the excitation frequency, for different local minima.

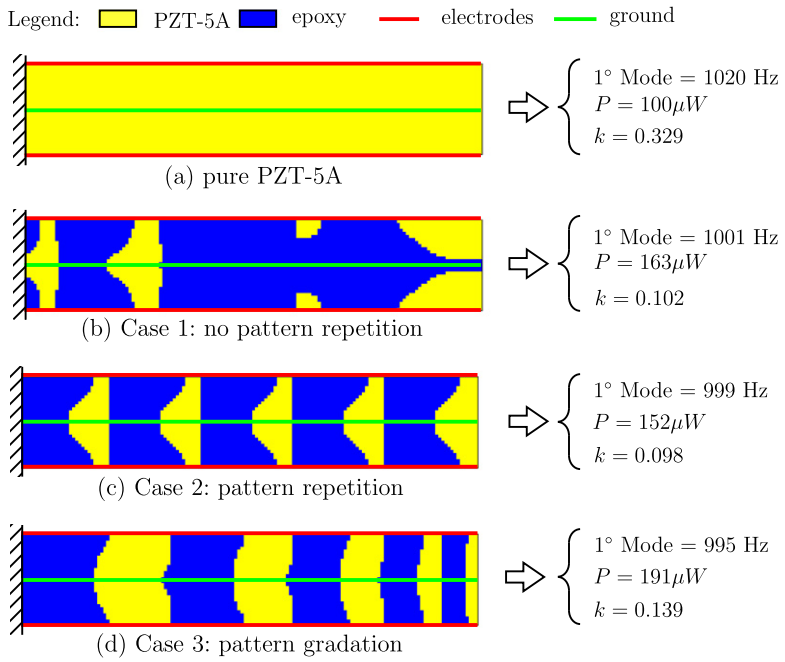

Fig. 13. Best performances for each case.

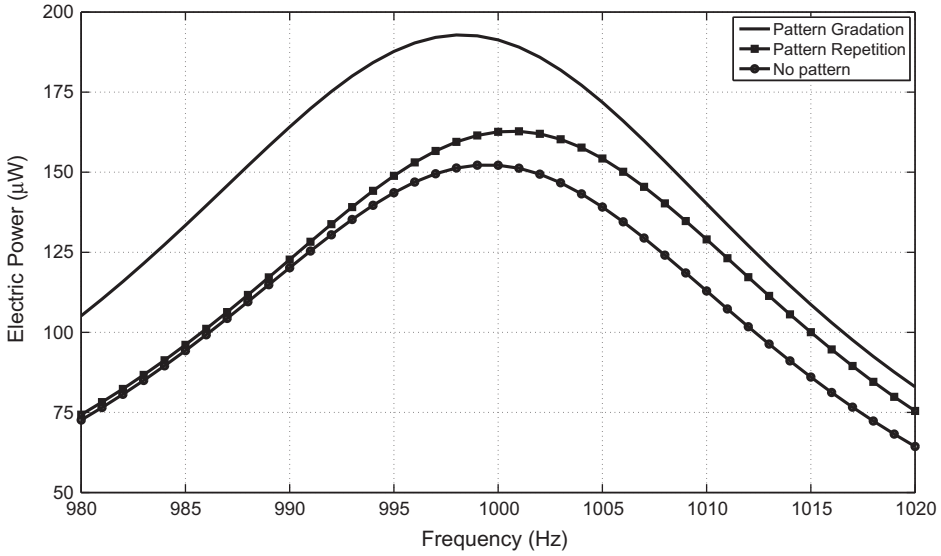

Fig. 14. Electric power generated in the load resistor as a function of excitation frequency.

resonance frequency is 995 Hz, which is the farthest from the excitation frequency of all three cases, and the electric power generated is 191 μW, achieving a gain of 91% with respect to the pure PZT-5A. From these results, it can be seen that the highest value of the electric power generated in the load resistor is obtained with the pattern gradation constraint, even though this design domain presents a smaller solution space in relation to the first case. It shows that, once the optimization of the dynamic problem has many local minima, the pattern gradation constraint can be used to modify the solution space, so a better local minima can be achieved.

An important aspect to be evaluated is the response of the electric power generated as a function of the excitation frequency, shown in Fig. 14. From this graphic it is clear that, although the optimized result obtained with pattern gradation constraint presents a difference of 5 Hz with respect to the excitation frequency, even when the structure is excited with a force operating at 1 kHz, this case generates the highest electric power.

6. Concluding remarks

This paper studies the influence of pattern gradation in the design of vibrating piezoelectric energy harvesting devices, based on bending behavior, using topology optimization. Maximization of the electric power presents many local minima, making it difficult to obtain the global optimum. From the numerical results presented, it can be seen that the highest value of the electric power generated in the load resistor is obtained with the pattern gradation constraint, even though this design domain presents a smaller solution space. Because the optimization of the dynamic problem has many local minima, the pattern gradation constraint modifies the solution space and guides the problem toward a more stable solution, so a better local minima can be achieved. In addition, the difference between the performance obtained with pattern repetition and pattern gradation resides in the electromechanical coupling coefficient k, whose values show that more efficient energy conversion is obtained with the pattern gradation constraint. As future work, new parameters can be added as design variables to the design of piezocomposite energy harvesting devices, such as the number of patterns and the variation of the pattern dimensions along the design domain.

Acknowledgments

The first author thanks FAPESP (São Paulo State Foundation Research Agency) by supporting him in his graduate studies through the fellowship No. 2008/57086-6. The third author is thankful for the financial support received from CNPq (National Council for Research and Development, Brazil), Nos. 303689/2009-9 and 562923/2008, and FAPESP Research Project No. 2001/02387-4. The authors also thank Prof. Svanberg for providing the source code for the Method of Moving Asymptotes (MMA).

References

[1] Erturk A, Renno JM, Inman DJ. Modeling of piezoelectric energy harvesting from an l-shaped beam-mass structure with an application to UAVS. J Intell Mater Syst Struct 2009;20:529–44.
[2] Anton SR, Sodano HA. A review of power harvesting using piezoelectric materials (2003–2006). Smart Mater Struct 2007;16:R1–R21.
[3] Priya S. Advances in energy harvesting using low profile piezoelectric transducers. J Electroceram 2007;19:165–82.
[4] Cook-Chennault KA, Thambi N, Sastry AM. Powering MEMS portable devices – A review of non-regenerative and regenerative power supply systems with special emphasis on piezoelectric energy harvesting systems. Smart Mater Struct 2008;17:043001.
[5] Silva ECN, Fonseca JSO, de Espinosa FM, Crumm AT, Brady GA, Halloran JW, et al. Design of piezocomposite materials and piezoelectric transducers using topology optimization – Part I. Arch Comput Methods Eng 1999;6:117–82.
[6] Rupp CJ, Evgrafov A, Maute K, Dunn ML. Design of piezoelectric energy harvesting systems: a topology optimization approach based on multilayer plates and shells. J Intell Mater Syst Struct 2009;20:1923–39.
[7] Zhu M, Worthington E, Njuguna J. Analyses of power output of piezoelectric energy-harvesting devices directly connected to a load resistor using a coupled piezoelectric-circuit finite element method. IEEE Trans Ultrasonics Ferroelect Frequency Control 2009;56:1309–18.
[8] Silva ECN, Fonseca JSO, Kikuchi N. Optimal design of periodic piezocomposites. Comput Methods Appl Mech Eng 1998;159:49–77.
[9] Silva ECN, Nishiwaki S, Kikuchi N. Design of piezocomposite materials and piezoelectric transducers using topology optimization – Part II. Arch Comput Methods Eng 1999;6:191–222.
[10] Sigmund O, Torquato S, Aksay IA. On the design of 1-3 piezocomposites using topology optimization. J Mater Res 1998;13:1038–48.
[11] Buehler MJ, Bettig B, Parker GG. Topology optimization of smart structures using a homogenization approach. J Intell Mater Syst Struct 2004;15:655–67.
[12] Jayachandran KP, Guedes JM, Rodrigues HC. Piezoelectricity enhancement in ferroelectric ceramics due to orientation. Appl Phys Lett 2008;92:232901.
[13] Jayachandran KP, Guedes JM, Rodrigues HC. Homogenization of textured as well as randomly oriented ferroelectric polycrystals. Comput Mater Sci 2009;45:816–20.
[14] Jayachandran KP, Guedes JM, Rodrigues HC. Stochastic optimization of ferroelectric ceramics for piezoelectric applications. Struct Multidiscip Optimiz 2011;44:199–212.

[15] Zheng B, Chang CJ, Gea HC. Topology optimization of energy harvesting devices using piezoelectric materials. Struct Multidiscip Optimiz 2009;38:17–23.
[16] Chen SK, Gonella S, Chen W, Liu WK. A level set approach for optimal design of smart energy harvesters. Comput Methods Appl Mech Eng 2010;199:2532–43.
[17] Nakasone PH, Silva ECN. Dynamic design of piezoelectric laminated sensors and actuators using topology optimization. J Intell Mater Syst Struct 2010;21:1627–52.
[18] Lee S, Youn BD. A new piezoelectric energy harvesting design concept: multimodal energy harvesting skin. IEEE Trans Ultrasonics Ferroelectr Frequency Control 2011;58:629–45.
[19] El-Sabbagh A, Baz A. Maximization of the harvested power from piezoelectric bimorphs with multiple electrodes under dynamic excitation. Finite Elements Anal Des 2011;47:1232–41.
[20] Stromberg LL, Beghini A, Baker WF, Paulino GH. Application of layout and topology optimization using pattern gradation for the conceptual design of buildings. Struct Multidiscip Optimiz 2011;43:165–80.
[21] Sigmund O. On the design of compliant mechanisms using topology optimization. Mech Struct Mach 1997;25:495–526.
[22] Bourdin B. Filters in topology optimization. Int J Numer Methods Eng 2001;50:2143–58.
[23] Guest JK, PrTvost JH, Belytschko T. Achieving minimum length scale in topology optimization using nodal design variables and projection functions. Int J Numer Methods Eng 2004;61:238–54.
[24] Sigmund O. Morphology-based black and white filters for topology optimization. Struct Multidiscip Optimiz 2007;33:401–24.
[25] Xu SL, Cai YW, Cheng GD. Volume preserving nonlinear density filter based on heaviside functions. Struct Multidiscip Optimiz 2010;41: 495–505.
[26] Kawamoto A, Matsumori T, Yamasaki S, Nomura T, Kondoh T, Nishiwaki S. Heaviside projection based topology optimization by a PDE-filtered scalar function. Struct Multidiscip Optimiz 2011;44:19–24.
[27] Guest JK. Topology optimization with multiple phase projection. Comput Methods Appl Mech Eng 2009;199:123–35.
[28] Wang FW, Lazarov BS, Sigmund O. On projection methods, convergence and robust formulations in topology optimization rid a-5354-2008. Struct Multidiscip Optimiz 2011;43:767–84.
[29] Cherkaev A. Variational methods for structural optimization, vol. 140. New York: Springer; 2000.
[30] Allaire G. Shape optimization by the homogenization method, vol. 146. New York: Applied mathematical sciences; 2002.
[31] Bendsoe MP, Sigmund O. Topology optimization – theory, methods and applications. New York, EUA: Springer; 2003.
[32] Svanberg K. The method of moving asymptotes – a new method for structural optimization. Int J Numer Methods Eng 1987;24:359–73.
[33] Nguyen TH, Paulino GH, Song J, Le CH. A computational paradigm for multiresolution topology optimization (MTOP). Struct Multidiscip Optimiz 2010;41:525–39.